DOI: 10.1002/chem.200901983

Computationally Designed Families of Flat, Tubular, and Cage Molecules Assembled with "Starbenzene" Building Blocks through Hydrogen-Bridge Bonds

Yan-Bo Wu,[a, b] Jin-Liang Jiang,[a] Ren-Wu Zhang,[c] and Zhi-Xiang Wang*[a]

Abstract: Using density functional calculations, we demonstrate that the planarity of the nonclassical planar tetracoordinate carbon (ptC) arrangement can be utilized to construct new families of flat, tubular, and cage molecules which are geometrically akin to graphenes, carbon nanotubes, and fullerenes but have fundamentally different chemical bonds. These molecules are assembled with a single type of hexagonal blocks called starbenzene (D_{6h} $C_6Be_6H_6$) through hydrogen-bridge bonds that have an average bonding energy of 25.4–33.1 kcal mol^{-1}. Starbenzene is an aromatic molecule with six π electrons, but its carbon atoms prefer ptC arrangements rather than the planar trigonal sp^2 arrangements like those in benzene. Various stability assessments indicate their excellent stabilities for experimental realization. For example, one starbenzene unit in an infinite two-dimensional molecular sheet lies on average 154.1 kcal mol^{-1} below three isolated linear $C_2Be_2H_2$ (global minimum) monomers. This value is close to the energy lowering of 157.4 kcal mol^{-1} of benzene relative to three acetylene molecules. The ptC bonding in starbenzene can be extended to give new series of starlike monocyclic aromatic molecules (D_{4h} $C_4Be_4H_4^{2-}$, D_{5h} $C_5Be_5H_5^-$, D_{6h} $C_6Be_6H_6$, D_{7h} $C_7Be_7H_7^+$, D_{8h} $C_8Be_8H_8^{2-}$, and D_{9h} $C_9Be_9H_9^-$), known as starenes. The starene isomers with classical trigonal carbon sp^2 bonding are all less stable than the corresponding starlike starenes. Similarly, lithiated $C_5Be_5H_5$ can be assembled into a C_{60}-like molecule. The chemical bonding involved in the title molecules includes aromaticity, ptC arrangements, hydrogen-bridge bonds, ionic bonds, and covalent bonds, which, along with their unique geometric features, may result in new applications.

Keywords: aromaticity · cage nanomolecules · density functional calculations · flat nanomolecules · planar tetracoordinated carbon

Introduction

Fullerenes,[1] carbon nanotubes,[2] and graphenes[3] have intrigued scientists from various fields due to their promising applications. The planarity of sp^2 carbon (sp^2C) is crucial for the planar structures of graphenes. As an exception to the traditional hybridization bonding of carbon, planar tetracoordinate carbon (ptC),[4] in which a carbon atom and its four bound atoms are in the same plane, has recently received increasing attention.[5] No doubt, the tetrahedron is generally the most favorable geometric arrangement for four atoms bonded to a carbon atom. However, ptC can be achieved electronically,[4,6] mechanically,[4,7] or by a combination of both.[8] Molecules or species with ptC arrangements were not only computationally designed, whereby some ptC species were even characterized as the global minima,[9] but also experimentally synthesized.[9d–h,10] Planar carbon arrangements with coordination numbers greater than four have also been explored.[9b,c,11] Can the planarity of ptC arrangement be utilized to build molecules similar to graphenes, or even to carbon nanotubes and fullerenes? Using ptC arrangements to construct solids[12] or other types of molecules has previously been reported.[13] Highlights related to the current study include the nanoribbons and nanotubes constructed from ptC CM_4H_4 (M = Ni, Pd, and Pt)[13l,14] and

[a] Dr. Y.-B. Wu, J.-L. Jiang, Prof. Z.-X. Wang
College of Chemistry and Chemical Engineering
Graduate University of Chinese Academy of Sciences
Beijing, 100049 (China)
Fax: (+86) 10-8825-6693
E-mail: zxwang@gucas.ac.cn
zxwangli@gmail.com

[b] Dr. Y.-B. Wu
Institute of Molecular Science, Key Laboratory of Chemical Biology and Molecular Engineering of Education Ministry
Shanxi University, Taiyuan, 030006, Shanxi (China)

[c] Prof. R.-W. Zhang
Department of Physical Science, Southern Utah University
Cedar, UT 84720, Utah State (USA)

Supporting information for this article is available on the WWW under http://dx.doi.org/10.1002/chem.200901983.

$C_3B_2H_4$,[13g,h,15] and B_2C-based sheets and nanotubes.[9c,13m] We herein report our computational predictions of new families of flat, tubular, and cage molecules that are geometrically akin to, but have chemical bonds fundamentally different from, their sp^2C counterparts. As will be shown, the new families of nanomolecules are also different from the previously reported ptC-constructed nanomolecules.

Results and Discussion

Starbenzene: the building block: The present quest originated from a different perspective in interpreting the structure of polybenzenoid hydrocarbons (e.g., $C_{42}H_{18}$ in Scheme 1 A).

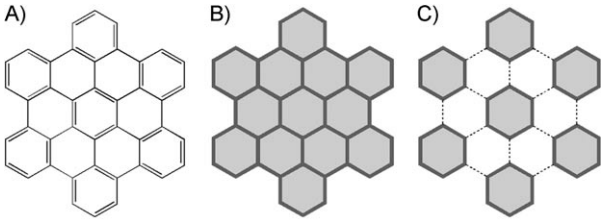

Scheme 1. Two perspectives of polybenzenoid hydrocarbons (A): Viewed as fused hexagonal blocks sharing CC edges (B) and as separated hexagonal blocks bonded by interblock bonds (C).

While they are often viewed as C_6 hexagons fused by sharing CC edges (Scheme 1 B), we decompose them into discrete hexagonal blocks linked by interblock bonds (Scheme 1 C). The number of atoms in the hexagonal block is not necessarily limited to six, and regular hexagons of any number of atoms can fulfill the geometric requirement to fill a plane without rifts.

Based on Scheme 1 C and our goal to achieve ptC-constructed title nanomolecules, we searched for suitable hexagonal blocks that meet the following criteria: 1) all carbon atoms adopt ptC arrangements; 2) the blocks are able to bond to their neighbors to form large assemblies; 3) the blocks should be neutral to avoid high net charges when they are assembled together; and 4) they should be minima on their potential-energy surfaces (PES) and thus have reasonable stability for experimental realization. With regard to criterion 4, it would be ideal if the blocks were global minima and also meet criteria 1–3. However, we did not consider being a global minimum as an indispensable criterion, because interblock bonding can lower the energy and thus benefit the stability of the whole system, when the blocks are bonded together. To our knowledge, no global minimum which meets criteria 1–3 has been reported.

The D_{6h} C_6Li_6 with six ptCs, which has been characterized computationally to be a minimum (not a global minimum),[16] is a candidate. Experimentally, a peak corresponding to the C_6Li_6 cation with C_6 ring was also observed in the high-resolution mass spectrum, though the structure of the species was not determined.[17] According to Scheme 1 C, we considered two forms of planar molecules (A and B in Figure 1) assembled from seven C_6Li_6 monomers. In form A, all atoms are placed in the same plane, giving a D_{6h} $(C_6Li_6)_7$ complex. Geometric optimization drove the complex apart, and the optimized structure is a 12th-order

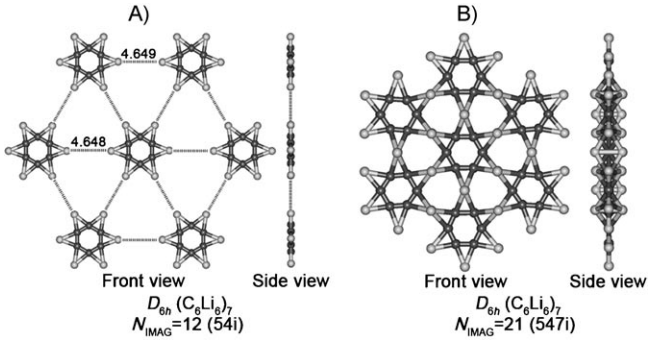

Figure 1. Optimized structures of two forms of D_{6h} $(C_6Li_6)_7$ complexes, together with the numbers of imaginary frequencies (N_{IMAG}) and the largest imaginary frequencies [cm^{-1}] in parentheses. Color versions of the figures in this paper are given in the Supporting Information (SI9).

saddle point. The small complexation energy (8.3 kcal mol^{-1}) and the large interblock distance ($R_{Li\cdots Li}$ = 4.648/4.649 Å) reflect that no interblock bonds are formed. Consistently, natural bond orbital (NBO) analysis[18] on a D_{6h} C_6Li_6 monomer revealed that each Li atom bears a positive charge of 0.57 e and has a total Wiberg bond index (WBI) of 0.84. The positive charges result in intermolecular Coulomb repulsions that separate the monomers, whereas the WBI implies that Li nearly exhausts its bonding capability. Therefore, it is not able to bond to nearby blocks efficiently in form A. In form B of $(C_6Li_6)_7$, the Li atoms are positioned perpendicular to the plane of the complex to bridge the C_6 units together. Although the optimized structure lies 189.0 kcal mol^{-1} below the seven isolated monomers, it has twenty-one imaginary frequencies, and sixteen of them tend to destroy its planar geometry. Our previously designed "hyparene" representative, D_{2h} C_6B_6,[11b] was also considered. To meet the geometric requirement, we modified D_{2h} C_6B_6 to a D_{6h} block with six ptCs. However, D_{6h} C_6B_6 is a sixth-order saddle point and 297.0 kcal mol^{-1} higher in energy than the D_{2h} minimum, which excludes its candidacy as a building block.

We recently found that the BeH group is an appropriate ligand to stabilize ptC,[19] which, along with the isolobal relationship of BeH to Li, suggested our replacing the six Li atoms in C_6Li_6 with BeH groups. We also expected that the electron deficiency of BeH group would result in intermolecular hydrogen-bridge (H-bridge) bonds similar to that in BeH_2 dimer to meet criterion 2. The reasoning was proved to be feasible by quantum mechanics calculations. Calculations at various levels (see SI1-Table 1 in the Supporting Information) verified that D_{6h} $C_6Be_6H_6$ (**1** in Figure 2), named starbenzene after its starlike geometry, is a minimum. Its sp^2C isomer **2** with classic Lewis structure is a first-order saddle point and 24.3 kcal mol^{-1} higher in energy than **1** at the B3LYP/6-31G* + ΔZPE level and 29.4 kcal mol^{-1} higher

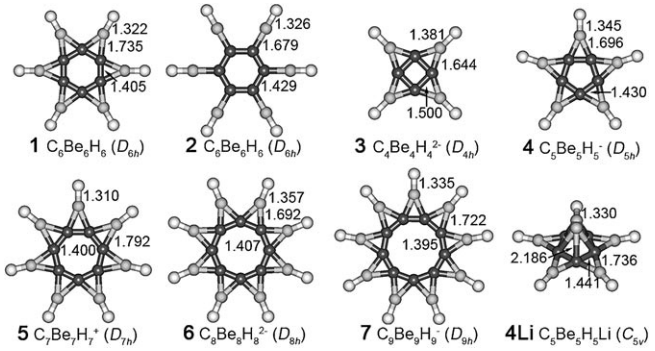

Figure 2. Optimized structures of **1**–**7** and **4Li** together with key bond lengths [Å].

at the CCSD(T)/cc-pVTZ//MP2/cc-pVTZ+ΔZPE(MP2) level.

Although the BeH groups in **1** have empty p_z atomic orbitals available to accept electrons from the C_6 ring, **1** has three π molecular orbitals identical to those in benzene (Figure 3A). Quantitatively, the total π occupancies on the

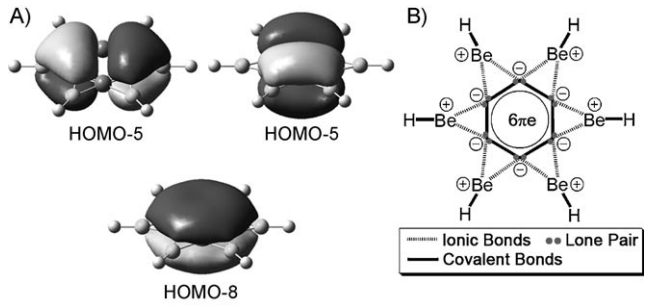

Figure 3. Three π orbitals of starbenzene (A) and simplified model for its electronic structure (B).

six beryllium atoms and on the six carbon atoms given by NBO analysis are 0.10 and 5.87 e, respectively. Therefore, starbenzene is an aromatic system with six π electrons. As shown in Table 1 and 2, the aromatic character of **1** is also manifested in the C–C bond lengths (1.405 Å), the C–C Wiberg bond indices (1.42), and the negative nucleus-independent chemical shift [NICS(1 Å)][20] (−10.9 ppm). These values compare with 1.391 Å, 1.44, and −7.8 ppm for benzene, respectively. The large charge separations (Q_C = −0.86 e and Q_{Be} = +1.35 e) and the small WBI values (0.13) of the C–Be bonds suggest that the C–Be bonds are predominately ionic. Based on the above analyses, we propose a simplified model for the electronic structure of starbenzene (Figure 3B). Apparently, positioning the BeH groups in the bridging positions can maximize the ionic interactions and therefore energetically benefit **1** over isomer **2**.

The ptC bonding in **1** can be extended; the monocyclic aromatic hydrocarbons ($C_4H_4^{2-}$, $C_5H_5^-$, $C_7H_7^+$, $C_8H_8^{2-}$, and $C_9H_9^-$) all have BeH-substituted counterparts (Figure 2). Table 1 compares the geometric and energetic data of these ptC molecules and their sp^2C isomers. All of the ptC molecules are lower in energy than their respective sp^2C isomers, and only the sp^2C isomer of **3** is a minimum. The energy differences between the two isomers in the cases of **6** and **7**, which are as large as 169.9 and 175.6 kcal mol^{-1}, respectively, further magnify the preference for ptC over sp^2C bonding in such molecules. Their NICS(1 Å) values and NBO results analyses of **3**–**7** are included in Table 2. The total π occupancies on the central carbon rings of **3**–**7** of 6 or 10 are close to the $4n+2$ π electron counts. Consistently, **3**–**7** have C–C bond lengths, NICS(1 Å), and C–C WBIs comparable to those of their respective monocyclic hydrocarbons. Taking the net charges of **3**–**7** into account, the NBO charge populations indicate that **3**–**7** can also be represented by a simplified model similar to Figure 3B but with 10 π electrons located on the central rings in the cases of **6** and **7**. Due to their aromatic characters and starlike geometries, we hereafter name this family of molecules starenes.

Designing ptC-containing nanomolecules: Among these starenes, starbenzene (**1**) is the desired block that can function like a jigsaw piece to be assembled together. By using the three linking patterns depicted in Figure 4, point-to-point (PP), edge-to-edge (EE), or a combination of both (PE), starbenzene monomers can be assembled into flat (F), tubular (T), and cage (C) molecules (Figure 5) through H-bridge bonds. For convenience with regard to the description, the nanomolecules reported in the following are designated as $MLLS_n$, where M, LL, S, and *n* represent the monomer block [**1**, **2**, or **4Li** (see below)], the linking pattern (PP, EE, or PE), the molecular shape (F, T, and C), and the number of monomers contained, respectively. Figure 5 only presents examples, and those not shown but mentioned in the text are given in the Supporting Information (SI2).

Planar molecules: Joining starbenzene pieces point-to-point (PP) gives flat (F) molecules (e.g., **1PPF$_{19}$** in Figure 5). The intermolecular H-bridge bonds glue starbenzene pieces to-

Table 1. Comparison of **1** and **3**–**7** with their sp^2C isomers, including the number of imaginary frequencies N_{IMAG}, smallest harmonic vibrational frequencies (SHVF) [cm^{-1}], bond lengths [Å], and the energy differences ΔE [kcal mol^{-1}] between two isomers.

	$C_6Be_6H_6$		$C_4Be_4H_4^{2-}$		$C_5Be_5H_5^-$		$C_7Be_7H_7^+$		$C_8Be_8H_8^{2-}$		$C_9Be_9H_9^-$	
	ptC	sp^2C	ptC	sp^2C	ptC	sp^2C	ptC	sp^2C	ptC	sp^2C	ptC	sp^2C
N_{IMAG}	0	1	0	0	0	1	0	5	0	8	0	11
SHVF	102	167*i*	153	48	112	26*i*	41	214*i*	81	464*i*	33	486*i*
R_{CC}	1.405	1.429	1.503	1.49	1.433	1.451	1.406	1.433	1.412	1.456	1.401	1.442
R_{CBe}	1.735	1.679	1.649	1.615	1.702	1.635	1.798	1.723	1.697	1.649	1.727	1.677
R_{BeH}	1.322	1.326	1.379	1.372	1.347	1.347	1.315	1.319	1.359	1.355	1.338	1.338
ΔE	0.0	24.3	0.0	32.3	0.0	26.4	0.0	3.7	0.0	169.9	0.0	175.6

Table 2. NICS (1 Å) values of **1** and **3**–**7** and NBO analysis results, which include natural atomic charges Q, Wiberg bond indices (WBI), and the total occupancies of π electrons of whole molecules (Tot), all carbon atoms (C_{all}), and all beryllium atoms (Be_{all}).

	R_{C-C}	NICS	Q			WBI					n_π	
			C	Be	H	C–C	C–H	C–Be	Be–H	Tot	C_{all}	Be_{all}
1	1.410	−13.7	−0.83	+1.35	−0.52	1.41		0.13	0.68	5.99	5.88	0.11
C_6H_6	1.397	−9.7	−0.24		+0.24	1.44	0.92			5.99	5.99	
3	1.503	−14.1	−1.22	+1.34	−0.62	1.18[a]		0.21	0.57	5.99	5.60	0.39
$C_4H_4^{2-}$	1.470	−7.8	−0.59		+0.09	1.23[a]	0.96			5.96	5.96	
4	1.433	−11.4	−0.99	+1.36	−0.57	1.37		0.16	0.63	5.99	5.79	0.20
C_5H_5-	1.415	−12.4	−0.37		+0.17	1.41	0.94			5.96	5.96	
5	1.406	−7.5	−0.70	+1.31	−0.47	1.40		0.12	0.72	5.99	5.92	0.07
$C_7H_7^+$	1.399	−9.7	−0.14		+0.28	1.41	0.89			5.99	5.99	
6	1.412	−13.4	−0.99	+1.33	−0.59	1.33		0.18	0.59	9.98	9.59	0.39
$C_8H_8^{2-}$	1.418	−14.2	−0.39		+0.14	1.35	0.95			9.97	9.97	
7	1.401	−12.3	−0.87	+1.30	−0.54	1.38		0.17	0.63	9.98	9.73	0.25
$C_9H_9^-$	1.404	−13.5	−0.30		+0.19	1.40	0.93			9.98	9.98	

[a] For these molecules, the WBIs of the diagonal C–C bonds are large (0.24 and 0.29, respectively).

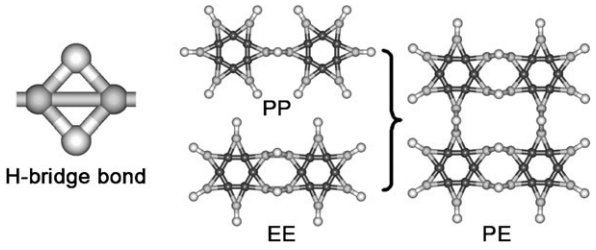

Figure 4. Illustrations of H-bridge bond and PP, EE, and PE linking patterns used to assemble starbenzene monomers into nanomolecules.

gether. Each hexagonal block in this type of flat molecules (see **1PPF$_{19}$**) except for those on the verges links to six neighbors optimally, which arrange all the H-bridge bonds along the BeH directions and thus minimize the strain. Regardless of the size of the systems, the average bonding energy per H-bridge bond (E_{HBB}) remains nearly identical (see Table 3 and the Supporting Information SI3), being −33.7 (**1PPF$_2$**), −33.5 (**1PPF$_3$**), −33.3 (**1PPF$_7$**), and −33.1 kcal mol^{-1} (**1PPF$_{19}$**), which are larger than the dimerization energy (−27.8 kcal mol^{-1}) of BeH_2. As indicated by the complexation energy difference of 397.2 kcal mol^{-1} of **1PPF$_7$** versus 189.2 kcal mol^{-1} of form B of D_{6h} $(C_6Li_6)_7$, assembling starbenzene is much energetically favorable than assembling C_6Li_6.

The molecules constructed by PP linking exactly follow the linking pattern shown in Scheme 1C. Alternatively, starbenzene monomers can be joined edge-to-edge (EE) to give another type of flat molecules (e.g., **1EEF$_{16}$** in Figure 5), which are akin to [*n*]phenylene. The E_{HBB} values in **1EEF$_2$** (−28.7), **1EEF$_4$** (−28.0), **1EEF$_6$** (−27.9), **1EEF$_{10}$** (−27.6), and **1EEF$_{16}$** (−27.5 kcal mol^{-1}) are less than that of about 33.0 kcal mol^{-1} in the PP-fused flat molecules, and reflect the higher strain of EE than PP fusions.

The PP and EE fusions can be combined to construct the third type of flat molecules (e.g., **1PEF$_{16}$**). As expected, because the PE fusion contains both PP and EE patterns, the E_{HBB} values in PE-fused molecules lie between those of PP and EE fusions: the E_{HBB} values of 29.9 in 2×2 PE-fused **1PEF$_4$**, 29.5 in 3×3 PE-fused **1PEF$_9$**, and 29.4 kcal mol^{-1} in 4×4 PE-fused **1PEF$_{16}$** compare with 33.1 and 27.5 kcal mol^{-1} in PP- and EE-fused molecules, respectively.

Tubular molecules: The flat molecules can be rolled into molecular tubes (T). To be computationally affordable and as a demonstration, we only considered examples in which each layer consists of six starbenzene monomers. The one-, two-, and three-layered tubes, **1PPT$_{6*1}$**, **1PPT$_{6*2}$** and **1PPT$_{6*3}$** (Figure 5), obtained by rolling PP-fused flat molecules, were verified to be minima. Understandably, the geometric confinement due to tubular geometry bends the ptCs away from a plane slightly. Relative to the flat molecules, the bending strain reduces their E_{HBB}: the values of −28.4 (**1PPT$_{6*1}$**), −30.1 (**1PPT$_{6*2}$**), and −30.2 kcal mol^{-1}(**1PPT$_{6*3}$**) are less than that in the PP-fused flat molecules (ca. 33.0 kcal mol^{-1}). The E_{HBB} can be expected to approach that of the flat molecule as the diameter of the tube increases.

A PE-fused sheet (e.g., **1PEF$_{16}$**) can be rolled into two types of nanotubes. Rolling the PE-fused sheet horizontally and vertically gives 1PE$_h$T- and 1PE$_v$T-type nanotubes, respectively, which correspond to (*n*,0) and (0,*m*) carbon nanotubes, respectively. The one-, two-, and three-layered nanotubes, **1PE$_h$T$_{6*1}$**, **1PE$_h$T$_{6*2}$**, **1PE$_h$T$_{6*3}$**, **1PE$_v$T$_{6*2}$**, **1PE$_v$T$_{6*2}$**, **1PE$_v$T$_{6*2}$**, and **1PE$_v$T$_{6*3}$** are all energy minima. Figure 5 includes the representatives **1PE$_h$T$_{6*3}$** and **1PE$_v$T$_{6*3}$**. Similar to the PP-fused tubes, the E_{HBB} values of **1PE$_h$T$_{6*3}$** and **1PE$_v$T$_{6*3}$** of 27.6 and 26.0 kcal mol^{-1}, respectively, are lower than that of the PE-fused flat molecules (29.3 kcal mol^{-1}). The larger E_{HBB} of PE$_h$-type tubes compared to PE$_v$-type tubes is due to the larger fraction of EE fusions in the latter.

Because PP fusion is energetically more favorable than EE and PE fusions, we further considered the possibility to use **2** as a basic block to build PP-fused flat and tubular molecules, even though **2** is not a minimum. The **2**-based structures **2PPF$_7$** and **2PPT$_{6*2}$** were optimized (Figure 6). They are 28th- and 13th-order saddle points and 308.7 and 382.2 kcal mol^{-1} higher in energy than **1PPF$_7$** and **1PPT$_{6*2}$**, respectively. This indicates that polymerization is not able to

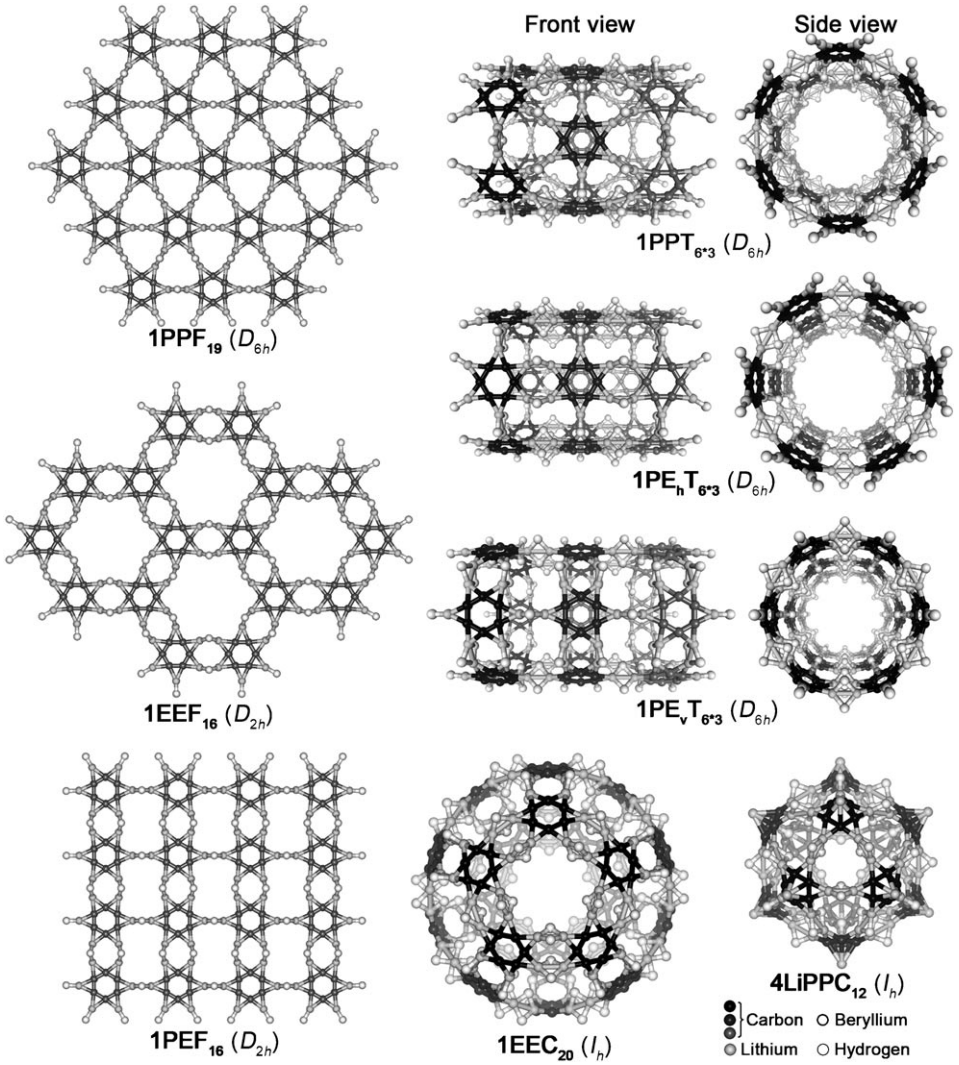

Figure 5. Optimized structures of representatives of flat, tubular, and cage nanomolecules. Different colors represent carbon atoms in the different positions for clear views of tubular and cage molecules.

alter the preference of ptC over sp^2C bonding in starbenzene.

Flat and tubular molecules constructed from ptC blocks have been previously reported: by eliminating the outlying substituents (e.g., H atoms), building blocks are condensed to give nanomolecules. Unlike the condensation building strategy, starbenzene monomers are assembled just like a jigsaw puzzle, without losing any substituents while maintaining the integrity of the individual blocks. Because starbenzene has a large HOMO–LUMO gap (4.6 eV) and the integrity of each starbenzene monomer is maintained, our nanomolecules have much larger HOMO–LUMO gaps (>4.30 eV, see Table 1), as opposed to less than 3.23 eV for CM_4H_4-based systems (M=Ni, Pd, and Pt),[13] less than 0.55 eV for $C_3B_2H_4$-based tubes,[13g] and zero band gap for B_2C-based flat and tubular molecules.[13m] Furthermore, the HOMO–LUMO gaps of our molecules only change slightly as the molecular size increases. In contrast, the HOMO–LUMO gaps of the previously reported ptC-based nanomolecules, as well as those of the graphenes and carbon nanotubes built by conventional carbon bonding, often decrease gradually.

Cage molecules: The flat and tubular molecules inevitably have dangling BeH groups at their verges. However, the BeH groups can be fully utilized to form cage (C) molecules. For example, twenty starbenzene monomers can be assembled to give a molecular ball with I_h symmetry via EE linking (**1EEC$_{20}$**, Figure 5). Referring to C_{60}, the twenty $C_6Be_6H_6$ fragments correspond to the twenty hexagons in

Table 3. Point groups (PG), smallest harmonic vibrational frequencies (SHVF) [cm^{-1}], HOMO–LUMO gaps (GAP) [eV], binding energy per H-bridge bond (E_{HBB}) [kcal mol^{-1}], energy lowering per starbenzene unit relative to isolated starbenzene (E_{LPS}) [kcal mol^{-1}], and minimum and maximum lengths [Å] of C–C, C–Be, interblock Be–Be, and Be–H (H-bridge) bonds.

	PG	SHVF	GAP	E_{HBB}	E_{LPS}	R_{C-C}[a] (min./max.)	R_{C-Be} (min./max.)	R_{Be-Be}[b] (min./max.)	R_{Be-H}[b] (min./max)
1	D_{6h}	101	4.53			1.410/1.410	1.739/1.739		
1PPF$_{19}$	D_{6h}	4	4.64	−33.1	−73.1	1.398/1.404	1.722/1.743	1.974/1.978	1.465/1.468
1EEF$_{16}$	D_{2h}	3	4.51	−27.5	−65.3	1.401/1.412	1.728/1.730	1.950/1.958	1.471/1.474
1PEF$_{16}$	D_{2h}	5	4.35	−29.3	−66.0	1.396/1.416	1.720/1.757	1.952/1.978	1.464/1.479
1PPT$_{6*3}$	D_{6h}	12	4.60	−30.2	−70.4	1.403/1.409	1.724/1.756	1.978/1.984	1.456/1.474
1PE$_h$T$_{6*3}$	D_{6h}	10	4.41	−27.6	−64.5	1.402/1.410	1.724/1.756	1.957/1.986	1.453/1.484
1PE$_v$T$_{6*3}$	D_{6h}	15	4.30	−26.0	−69.3	1.396/1.415	1.724/1.754	1.960/1.979	1.460/1.490
1EEC$_{20}$	I_h	32	4.79	−25.4	−76.2	1.403/1.403	1.738/1.739	1.959/1.959	1.465/1.465
4 LiEEC$_{12}$	I_h	72	3.94	−24.0	−60.1[c]	1.439/1.440	1.747/1.747	1.993/1.994	1.455/1.488

[a] R_{CC}=1.391 Å in benzene. [b] R_{BeBe}=2.003 and R_{BeH}=1.473 Å in BeH_2–BH_2. [c] Relative to **4 Li**.

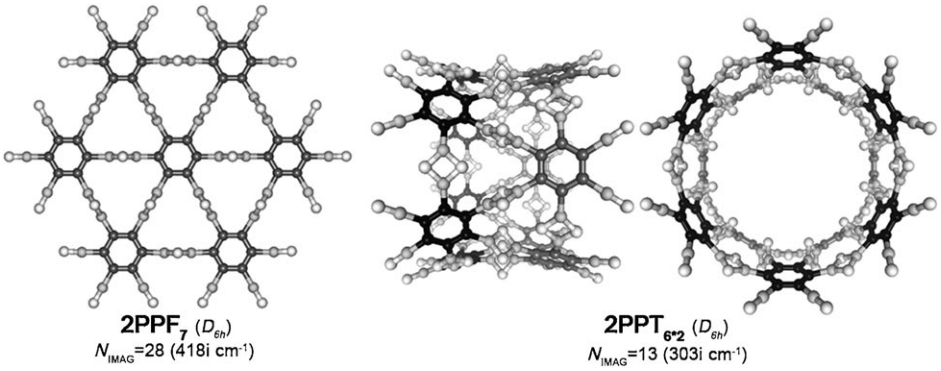

Figure 6. Optimized structures of **2PPF$_7$** and **2PPT$_{6*2}$**.

C_{60}, and the twelve pentagon holes, each of which is encompassed by five starbenzene monomers, to the twelve pentagons. Its E_{HBB} of -25.4 kcal mol^{-1}, which is lower than those of the EE-fused flat molecules, indicates the additional strain due to the cage geometry. Nevertheless, saturation of the H-bridge bonds can benefit the formation of cage molecules. The average energy per **1** unit in **1EEC$_{20}$** of 76.2 kcal mol^{-1} is less than that of a free **1** monomer. The value is the largest among those for the molecules considered (see column 6 in Table 3 and Supporting Information SI3).

The D_{5h} $C_5Be_5H_5^-$ (**4**) is not suitable to construct flat molecules, but can be used to build molecular cages. To be a building block, it must be neutralized to avoid high charges (meeting criterion 2). Lithiated $C_5Be_5H_5Li$ (**4Li**, a C_{5v} minimum) has six interstitial electrons for 3D aromaticity. By PP fusion, twelve **4Li** monomers can be assembled into the **4LiPPC$_{12}$** cage (Figure 5). Referring to C_{60}, **4LiPPC$_{12}$** is also consistent with the bonding pattern (Scheme 1C) although the block is not hexagonal; the twelve **4Li** units correspond to the hexagonal blocks, which are linked by H-bridge bonds. The pentagonal geometry of the block and the smaller size of **4LiPPC$_{12}$** compared to **1EEC$_{20}$**, make the E_{HBB} of **4LiPPC$_{12}$** (-24.0 kcal mol^{-1}) lower than that of -25.4 kcal mol^{-1} for **1EEC$_{20}$**. To our knowledge, no similar ptC-constructed molecule has been reported previously.

Stability considerations: The predicted molecules have regular bond lengths and large HOMO–LUMO gaps of 3.94–4.64 eV (see column 4 in Table 3 and Supporting Information SI3), but the smallest harmonic vibrational frequencies (SHVFs) are not large, to which we paid special attention. It is verified that the vibrations corresponding to the SHVFs are not local motions that destroy the planarity of the building blocks and reflect the flexibilities of the molecules as a whole (see the movies in Supporting Information SI4). The small SHVF values can be ascribed to the large sizes of the systems and that H-bridge bonds are weaker than covalent bonds. Note that $C_{42}H_{18}$ in Scheme 1A has two degenerate imaginary frequencies of $5i$ cm^{-1}.

To be experimentally attainable, the predicted molecules should have a certain degree of stability. Three prominent theoretical chemists[21] recently suggested guidelines to their colleagues for judging computed species to be viable. For such large systems, it is impracticable to investigate their stabilities by exploring their PESs. Because our molecules are pieced together from blocks and the integrities of the blocks are maintained, we investigated their stabilities by examining how tightly the building blocks are bonded together and how stable the building block itself is. The E_{HBB} values (24.0–33.0 kcal mol^{-1}) and the average counts of three such bonds for each block indicate that the blocks are bonded together tightly. It could be difficult to separate monomers from these predicted nanomolecules.

We now considered the stability of the starbenzene building block. Although our GXYZ random search[22] has been proved to be reliable for locating global minima for C_2E_4 (E = Al, Ga, In, and Tl) ptC species,[14] without any geometric restrictions, it is impractical to locate the global minimum for such systems containing three types of a total of eighteen atoms. Because the C_6 ring resembles the rigid benzene ring (Figure 3B), we first considered starbenzene isomers with the geometric restriction of having a C_6 ring. Combining the *GXYZ* random search and manual constructions, we located twenty-six such isomers, none of which is lower in energy than **1** even though most of them have intramolecular H-bridge bonds. This is similar to the C_6Li_6 case; with the restriction of having a C_6 ring, the **1**-like D_{6h} structure of C_6Li_6 is 10.0 kcal mol^{-1} more stable than the nearest isomer at the B3LYP/6-311+G** level.[23] Figure 7 displays the structures of the lowest six isomers (**8**–**13**) after starbenzene and others are provided in Supporting Information SI5.

Based on the previous studies on C_6Li_6[16] and Si_6Li_6,[24] we further considered starbenzene isomers without a C_6 ring and manually built isomers **14**–**17**, similar to those of C_6Li_6 and Si_6Li_6. Their optimized structures are at least 64.7 kcal mol^{-1} higher than that of starbenzene. In the Si_6Li_6 case, a structure similar to **14** was predicted to be 47.7 kcal mol^{-1} lower in energy than D_{6h} Si_6Li_6 at the B3LYP/6-311+G(2d,p) level.[24a] In contrast, isomer **14** is 64.7 kcal mol^{-1} higher in energy than starbenzene. Alternatively, starbenzene can be viewed as a $C_2Be_2H_2$ trimer. We thus examined the stability of starbenzene relative to various $C_2Be_2H_2$ trimers. Extensive random search revealed that the linear form (**18A**) is the global minimum of $C_2Be_2H_2$ at the DFT/6-31G*, MP2/cc-pVTZ, and CCSD(T)/cc-pVTZ//MP2/cc-pVTZ levels and lies much lower than its two nearby isomers, **18B** and **18C.** Starbenzene is 54.8 kcal mol^{-1} more stable than three separate **18A** species. Due to the intermolecular H-bridge bonding in $C_2Be_2H_2$ trimers, the energy differences between starbenzene and trimers **19**–**23** decrease.

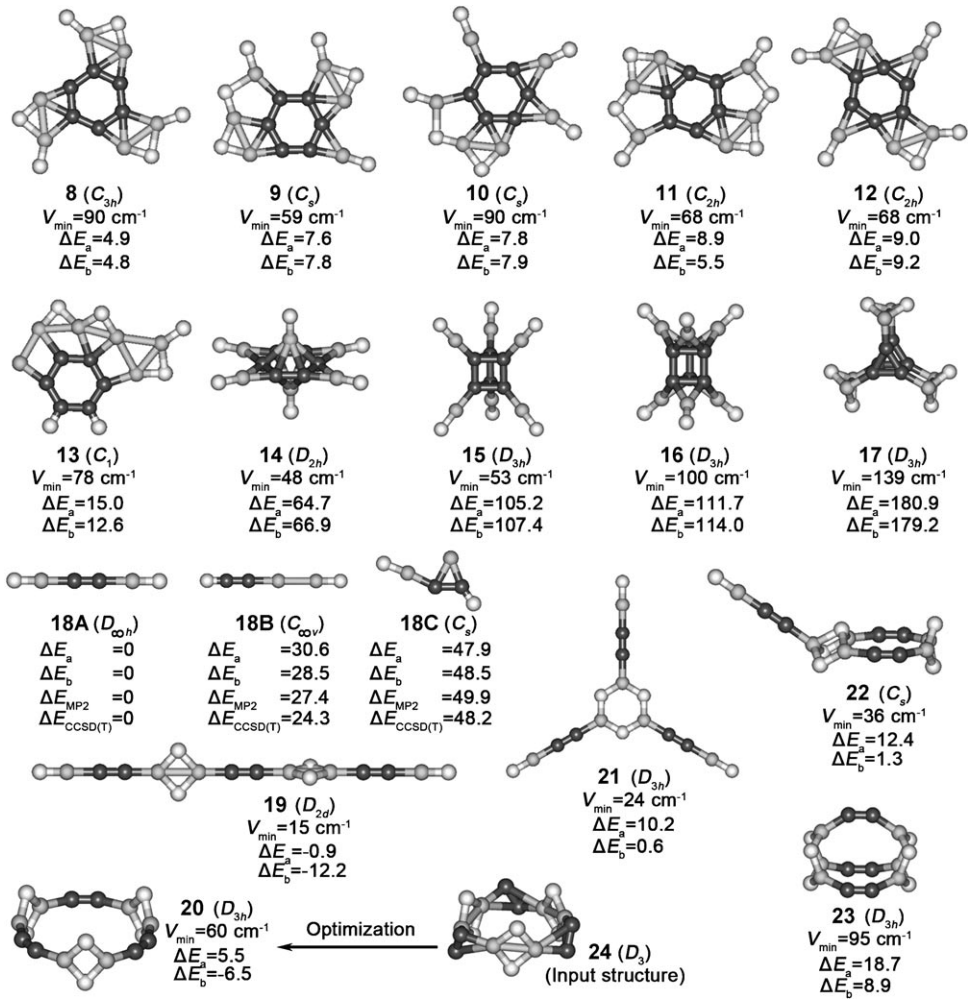

Figure 7. Optimized structures of the various isomers of starbenzene, together with the lowest vibrational frequencies V_{min} at the B3LYP/6-31G* level, and the energies relative to **1** at the B3LYP/6-31G* (ΔE_a) and B3LYP/6-311+G(3df,2p) (ΔE_b) levels. **18A**–**18C** are the three lowest isomers of $C_2Be_2H_2$ found by random research. The cc-pVTZ basis set was used for MP2 and CCSD(T)//MP2 calculations.

Starbenzene is 0.9 kcal mol^{-1} less stable than linear trimer **19**, but more stable than **20**–**23**. In the C_6Li_6 case, a D_3 structure was predicted to be 62.1 kcal mol^{-1} lower in energy than D_{6h} C_6Li_6 at the MP2/TZP level.[16b] However, geometric optimization on the D_3 C_6Li_6-like structure **24** gave the same structure as **20**, which is 5.5 kcal mol^{-1} less stable than **1**. To examine the reliability of the B3LYP/6-31G* results, we recalculated the isomers in Figure 7 at the B3LYP/6-311+G(3df,2p) level. As compared in Figure 7, the B3LYP/6-31G* calculations predict relative energies of isomers **8**–**17** in good agreement with the B3LYP/6-311+G(3df,2p) values, but underestimate those of trimers **19**–**23** by about 10.0 kcal mol^{-1}. Among all the considered isomers, **19** is the lowest lying and −12.2 kcal mol^{-1} [B3LYP/6-311+G(3df,2p)] more stable than starbenzene (starbenzene is thus not a global minimum). However, starbenzene blocks in our designed nanomolecules are not isolated and on average 64.5–76.2 kcal mol^{-1} (E_{LPS} in Table 3) lower in energy than a free starbenzene block due to intermolecular H-bridge bonding. Therefore, the starbenzene block in the designed nanomolecules still lies well below the located isomers though free starbenzene is not a global minimum. Moreover, the comparisons also imply that the B3LYP/6-31G* calculations may underestimate E_{LPS} in Table 3.

The stability of the building block was further examined by two sets of B3LYP/6-31G* Born–Oppenheimer molecular dynamics (BOMD)[25] simulations at 323 and 373 K, starting from **1**. The structural evolution (Figure 8) during the simulation shows that the starbenzene-like structures are well maintained in the 30 ps simulation. In the calculations of root mean square deviation (RMSD), starbenzene was used as the reference structure and hydrogen atoms were excluded. The dynamic simulations imply that there are no nearby low-lying isomers which can be visited by crossing low energy barriers. Furthermore, the two sets of simulations were run on the single monomer and did not include the stability effects due to the intermolecular H-bridge bonds. Therefore, the building block in the flat, tubular, and cage molecules should be more stable than an isolated monomer.

The above stability discussion is focused on the isolated starbenzene monomer, while the starbenzene monomers are

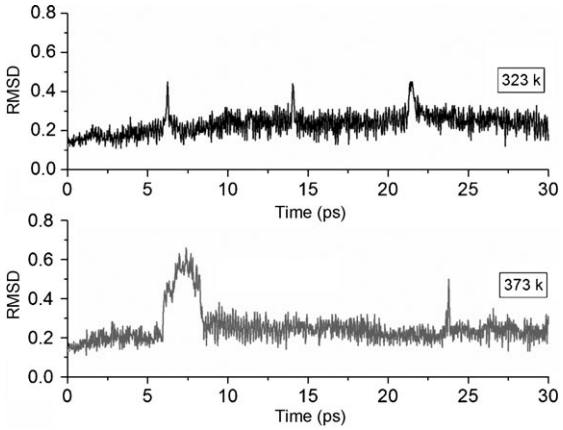

Figure 8. RMSD versus simulation time.

not isolated in the predicted nanomolecules and bonded together via H-bridge bonds with substantial bonding energy. As quantified by E_{LPS} (Table 3), a starbenzene block is on average 64.5–76.2 kcal mol^{-1} lower in energy than an isolated starbenzene monomer. Moreover, because of the relatively large fraction of dangling BeH groups in the given flat and tubular examples, the E_{LPS} values estimated from the size-limited systems do not properly account for the energetic benefits of H-bridge bonds in flat and tubular macromolecules. Using the linking patterns in Figure 4, one can extend the flat molecules to infinite two-dimensional (2D) sheets. The E_{LPS} values for infinite sheets **1PPF**$_\infty$, **1EEF**$_\infty$, and **1PEF**$_\infty$ approach thrice the E_{HBB} values, being 99.3, 82.5, and 87.9 kcal mol^{-1}, respectively, in comparison with values of 73.1 (**1PPF**$_{19}$), 65.3 (**1EEF**$_{16}$) and 66.0 kcal mol^{-1}(**1PEF**$_{16}$). For the tubular molecules, as the diameters and lengths of the tubes increase, the E_{LPS} values for **1PPT-**, and **1PE$_v$T-** and **1PE$_h$T-**type tubes should approach those of **1PPF**$_\infty$ and **1PEF**$_\infty$., respectively. Bearing in mind that **1PPF**$_\infty$ is more energetically favorable than other types of nanomolecules, we used **1PPF**$_\infty$ as an example to further discuss the stability of such infinite 2D sheets. Equation (1) estimates the average energy of one starbenzene block in **1PPF**$_\infty$ relative to three separated linear $C_2Be_2H_2$ monomers. Remarkably, the heat of formation of Equation (1) of 154.1 kcal mol^{-1} is very close to that of 157.4 kcal mol^{-1} for cyclization of three acetylene molecules to benzene [Eq. (2)]. The heat of formation of Equation (1) can be interpreted as the co-contributions due to forming starbenzene [54.8 kcal mol^{-1}, Eq. (3)] and three H-bridge bonds (99.3 kcal mol^{-1}). In comparison, energy release in acetylene cyclization is mainly due to formation of the C_6 ring. The difference between acetylene and $C_2Be_2H_2$ cyclization is that, while benzene is the final product of acetylene cyclization, $C_2Be_2H_2$ cyclization gives starbenzene, which can be further assembled into a large nanomolecule (i.e., **1PPF**$_\infty$) through H-bridge bonds. As three acetylene molecules can be "assembled" into a global minimum (benzene) by releasing 157.4 kcal mol^{-1} of energy, we wonder whether numerous $C_2Be_2H_2$ monomers can be assembled into "a global minimum" (**1PPF**$_\infty$) by releasing a similar average amount of energy (154.1 kcal mol^{-1}) per three $C_2Be_2H_2$ monomers. Unfortunately, it is impossible to provide direct evidence for this argument, but we call attention to the fact that $C_2Be_2H_2$ and C_2H_2 bear resemblance in terms of their electronic structures and the linear structures for their global minima.

$$3\,C_2Be_2H_2 \rightarrow \mathbf{1PPF}_n/n\ (n \rightarrow \infty) + 154.1\ \text{kcal mol}^{-1} \quad (1)$$

$$3\,C_2H_2 \rightarrow C_6H_6 + 157.4\ \text{kcal mol}^{-1} \quad (2)$$

$$3\,C_2Be_2H_2 \rightarrow \mathbf{1} + 54.8\ \text{kcal mol}^{-1} \quad (3)$$

It has been experimentally demonstrated that BeH_2 can be polymerized to give linear beryllium hydrides with H-bridge bonds.[26] Because $C_2Be_2H_2$ has a dimerization energy (27.8 kcal mol^{-1}, see below) nearly identical to that of BeH_2, we hypothesized that one-dimensional (1D) $C_2Be_2H_2$ chains could be one of the energetically favorable forms for $C_2Be_2H_2$ polymers. We thus examined the stabilities of the predicted molecules relative to 1D $C_2Be_2H_2$ chains. Calculations on 1D $(C_2Be_2H_2)_n$ (n=2–12) chains indicate that the E_{HBB} values for these polymers are almost identical (27.8 kcal mol^{-1}). We thus extrapolated the total energy of any length of 1D chain. The extrapolated energies show that planar **1PPF**$_{19}$, **1EEF**$_{16}$, and **1PEF**$_{16}$ are 869.9, 612.1, and 624.6 kcal mol^{-1}, tubular **1PPT**$_{6*3}$, **1PE$_h$T**$_{6*3}$, and **1PE$_v$T**$_{6*3}$, 778.1, 671.8, and 758.5 kcal mol^{-1}, and cage **1PPC**$_{20}$, 977.5 kcal mol^{-1} more stable than their corresponding 1D chain isomers. Note that this does not contradict the case of starbenzene versus $C_2Be_2H_2$ trimer because there is no H-bridge bond in starbenzene. It is not difficult to deduce that infinite 2D sheets or infinite tubes are much more energetically favorable than the 1D infinite $C_2Be_2H_2$ chain.

With regard to the experimental realization of starbenzene, we note that C_6Li_6 has been experimentally accessed by the reaction of hexachlorobenzene with *tert*-butyllithium. Starbenzene-like D_{6h} C_6Li_6 was computationally shown not to be the global minimum and the D_3 structure like **24** is more stable.[16b] However, considering the experimental temperature (−125 °C) and the rigid C_6 ring in hexachlorobenzene, the observed peak of the C_6Li_6 cation in the high-resolution mass spectrum probably originated from the starbenzene-like C_6Li_6, because formation of the D_3 structure requires breaking the C_6 ring of C_6Cl_6, and a previous study showed that the starbenzene-like C_6Li_6 is most stable among many C_6Li_6 isomers with a C_6 ring.[23] Note that our study also shows that starbenzene is most stable among $C_6Be_6H_6$ isomers with a C_6 ring.

Conclusions

We have computationally predicted new families of molecules similar to the well-known graphenes, carbon nanotubes, and fullerenes. The chemical bonds in these molecules are different from those carbon counterparts in embracing a bonding combination of aromaticity, ptC arrangements, H bridges, ionic bonds, and covalent bonds, which, along with their own geometric characteristics (see below), may result in new applications. In the concept illustrated by Scheme 1C, the covalent C–C bonds hold the C_6 hexagons together. Hydrogen-bridge bonding is well known, but using such bonds to build such-shaped molecules has not been explored. Since the H-bridge bond is weaker than a covalent bond and stronger than a hydrogen bond (the major forces for biological systems and biomimetic materials[27]), we speculate that this type of bond may also be used to build other similarly shaped molecules (i.e., not limited to having ptCs) which may play roles under conditions (e.g., as packing molecules) under which covalent bonds are too strong while hydrogen bonds are too weak. Currently, fullerenes and carbon nanotubes can only be generated under severe conditions. The predicted molecules are assembled from a

single type of building blocks, which may facilitate their experimental attainability in large quantities if the monomer can be synthesized. It is difficult to produce endofullerenes[28] by pouring guest species directly into cages. The large rings in **1EEC$_{20}$** or **4LiPPC$_{12}$** may facilitate pouring guest species directly into the cage to produce endofullerene-like molecules. The bridging atom is not limited to hydrogen. Other atoms and groups can play a similar role; fluorinated and chlorinated starbenzene-based molecules similar to **1PPF$_7$** are also minima (Supporting Information SI6). The chemistry revealed in this study may be extended to combinations of other group 2 and 4 elements. Stability assessments by various approaches indicate that they have excellent stabilities for experimental realization. To further encourage our experimental colleagues, we recall the famous C_{60} was predicted theoretically[29] before experimental discovery.[1] We invite experimental explorations into synthesis and potential applications.

Computational Section

Due to the large sizes of the studied systems (up to $C_{120}Be_{120}H_{120}$), DFT calculations at the B3LYP/6-31G* level were used to optimize the molecular structures and to verify the optimized structures to be minima by frequency analysis calculations. The relatively small molecules were recalculated at various more reliable levels (see Supporting Information SI1 for details), which gave geometric and energetic results in reasonable agreement with the B3LYP/6-31G* ones, indicating the suitability of the used theoretical level for the reported molecules. The B3LYP/6-31G* energetic results corrected for zero-point energies (ZPEs) are used in the discussion, unless otherwise specified. The Gaussian 03[30] package was used for all calculations.

Acknowledgements

This project is supported financially by Chinese Academy of Sciences, the NFSC (Grant No. 20973197), SXNFS (Grant No. 2009021016), and the China Postdoctoral Science Foundation (Grant No. 20090450608). The authors thank Mr. Hai-Gang Lu for technical support in using the GXYZ program.

[1] H. W. Kroto, J. R. Heath, S. C. Obrien, R. F. Curl, R. E. Smalley, *Nature* **1985**, *318*, 162–163.
[2] S. Iijima, *Nature* **1991**, *354*, 56–58.
[3] K. S. Novoselov, A. K. Geim, S. V. Morozov, D. Jiang, Y. Zhang, S. V. Dubonos, I. V. Grigorieva, A. A. Firsov, *Science* **2004**, *306*, 666–669.
[4] R. Hoffmann, R. W. Alder, C. F. Wilcox, Jr., *J. Am. Chem. Soc.* **1970**, *92*, 4992–4993.
[5] a) R. Keese, *Chem. Rev.* **2006**, *106*, 47874808; b) K. Sorger, P. von R. Schleyer, *J. Mol. Struct.* **1995**, *344–373*, 317–346; c) W. Siebert, A. Gunale, *Chem. Soc. Rev.* **1999**, *28*, 367–371; d) G. Merino, M. A. Mendez-Rojas, A. Vela, T. Heine, *J. Comput. Chem.* **2007**, *28*, 362–372.
[6] a) J. B. Collins, J. D. Dill, E. D. Jemmis, Y. Apeloig, P. v. R. Schleyer, R. Seeger, J. A. Pople, *J. Am. Chem. Soc.* **1976**, *98*, 5419–5427; b) G. Merino, M. A. Mendez-Rojas, A. Vela, *J. Am. Chem. Soc.* **2003**, *125*, 6026–6027; c) G. Merino, M. A. Mendez-Rojas, H. I. Beltraan, C. Corminboeuf, T. Heine, A. Vela, *J. Am. Chem. Soc.* **2004**, *126*, 16160–16169.
[7] a) D. R. Rasmussen, L. Radom, *Angew. Chem.* **1999**, *111*, 3051–3054; *Angew. Chem. Int. Ed.* **1999**, *38*, 2875–2878; b) L. Radom, D. R. Rasmussen, *Pure Appl. Chem.* **1998**, *70*, 1977–1984.
[8] a) Z. X. Wang, P. v. R. Schleyer, *J. Am. Chem. Soc.* **2001**, *123*, 994–995; b) Z. X. Wang, P. v. R. Schleyer, *J. Am. Chem. Soc.* **2002**, *124*, 11979–11982.
[9] a) Y. B. Wu, H. G. Lu, S. D. Li, Z. X. Wang, *J. Phys. Chem. A* **2009**, *113*, 3395–3402; b) Y. Pei, W. An, K. Ito, P. v. R. Schleyer, X. C. Zeng, *J. Am. Chem. Soc.* **2008**, *130*, 10394–10400; c) Y. Pei, X. C. Zeng, *J. Am. Chem. Soc.* **2008**, *130*, 2580–2592; d) X. Li, H. J. Zhai, L. S. Wang, *Chem. Phys. Lett.* **2002**, *357*, 415–419; e) X. Li, L. S. Wang, N. A. Cannon, A. I. Boldyrev, *J. Chem. Phys.* **2002**, *116*, 1330–1338; f) X. Li, H. F. Zhang, L. S. Wang, A. E. Kuznetsov, N. A. Cannon, A. I. Boldyrev, *Angew. Chem.* **2001**, *113*, 1919–1922; *Angew. Chem. Int. Ed.* **2001**, *40*, 1867–1870; g) X. Li, H. F. Zhang, L. S. Wang, G. D. Geske, A. I. Boldyrev, *Angew. Chem.* **2000**, *112*, 3776–3778; *Angew. Chem. Int. Ed.* **2000**, *39*, 3630–3633; h) X. Li, L. S. Wang, A. I. Boldyrev, J. Simons, *J. Am. Chem. Soc.* **1999**, *121*, 6033–6038; i) P. v. R. Schleyer, A. I. Boldyrev, *J. Chem. Soc. Chem. Commun.* **1991**, 1536–1538; j) W. Tiznado, N. Perez-Peralta, R. Islas, A. Toro-Labbe, J. M. Ugalde, G. Merino, *J. Am. Chem. Soc.* **2009**, *131*, 9426–9431.
[10] D. Röttger, G. Erker, *Angew. Chem.* **1997**, *109*, 840–856; *Angew. Chem. Int. Ed. Engl.* **1997**, *36*, 812–827.
[11] a) K. Exner, P. v. R. Schleyer, *Science* **2000**, *290*, 1937–1940; b) Z. X. Wang, P. v. R. Schleyer, *Science* **2001**, *292*, 2465–2469; c) R. M. Minyaev, T. N. Gribanova, A. G. Starikov, V. I. Minkin, *Dokl. Chem.* **2002**, *382*, 41–45; d) S. D. Li, G. M. Ren, C. Q. Miao, *Inorg. Chem.* **2004**, *43*, 6331–6333; e) S. Erhardt, G. Frenking, Z. F. Chen, P. v. R. Schleyer, *Angew. Chem.* **2005**, *117*, 1102–1106; *Angew. Chem. Int. Ed.* **2005**, *44*, 1078–1082; f) R. Islas, T. Heine, K. Ito, P. v. R. Schleyer, G. Merino, *J. Am. Chem. Soc.* **2007**, *129*, 14767–14774; g) K. Ito, Z. F. Chen, C. Corminboeuf, C. S. Wannere, X. H. Zhang, Q. S. Li, P. v. R. Schleyer, *J. Am. Chem. Soc.* **2007**, *129*, 1510–1511.
[12] a) P. D. Pancharatna, M. A. Mendez-Rojas, G. Merino, A. Vela, R. Hoffmann, *J. Am. Chem. Soc.* **2004**, *126*, 15309–15315; b) G. D. Geske, A. I. Boldyrev, *Inorg. Chem.* **2002**, *41*, 2795–2798.
[13] a) L. M. Yang, Y. H. Ding, C. C. Sun, *J. Am. Chem. Soc.* **2007**, *129*, 658–665; b) L. M. Yang, Y. H. Ding, C. C. Sun, *J. Am. Chem. Soc.* **2007**, *129*, 1900–1901; c) L. M. Yang, Y. H. Ding, W. Q. Tian, C. C. Sun, *Phys. Chem. Chem. Phys.* **2007**, *9*, 5304–5314; d) L. M. Yang, Y. H. Ding, C. C. Sun, *Theor. Chem. Acc.* **2008**, *119*, 335–342; e) L. M. Yang, H. P. He, Y. H. Ding, C. C. Sun, *Organometallics* **2008**, *27*, 1727–1735; f) L. M. Yang, X. P. Li, Y. H. Ding, C. C. Sun, *J. Mol. Model.* **2009**, *15*, 97–104; g) C. J. Zhang, W. X. Sun, Z. X. Cao, *J. Am. Chem. Soc.* **2008**, *130*, 5638–5639; h) W. X. Sun, C. J. Zhang, Z. X. Cao, *J. Phys. Chem. C* **2008**, *112*, 351–357; i) S. D. Li, J. C. Guo, C. Q. Miao, G. M. Ren, *Angew. Chem.* **2005**, *117*, 2196–2199; *Angew. Chem. Int. Ed.* **2005**, *44*, 2158–2161; j) S. D. Li, C. Q. Miao, G. M. Ren, J. C. Guo, *Eur. J. Inorg. Chem.* **2006**, 2567–2571; k) S. D. Li, C. Q. Miao, J. C. Guo, *J. Phys. Chem. A* **2007**, *111*, 12069–12071; l) Y. B. Wu, C. X. Yuan, F. Gao, H. G. Lu, J. C. Guo, S. D. Li, Y. K. Wang, P. Yang, *Organometallics* **2007**, *26*, 4395–4401; m) X. J. Wu, Y. Pei, X. C. Zeng, *Nano Lett.* **2009**, *9*, 1577–1582.
[14] S. D. Li, G. M. Ren, C. Q. Miao, Z. H. Jin, *Angew. Chem.* **2004**, *116*, 1395–1397; *Angew. Chem. Int. Ed.* **2004**, *43*, 1371–1373.
[15] T. N. Gribanova, R. M. Minyaev, V. I. Minkin, *Collect. Czech. Chem. Commun.* **1999**, *64*, 1780–1789.
[16] a) V. I. Minkin, R. M. Minyaev, A. G. Starikov, T. N. Gribanova, *Russ. J. Org. Chem.* **2005**, *41*, 1289–1295; b) B. J. Smith, *Chem. Phys. Lett.* **1993**, *207*, 403–406; c) Y. M. Xie, H. F. Schaefer, *Chem. Phys. Lett.* **1991**, *179*, 563–567.
[17] a) J. R. Baran, R. J. Lagow, *J. Am. Chem. Soc.* **1990**, *112*, 9415–9416; b) J. R. Baran, C. Hendrickson, D. A. Laude, R. J. Lagow, *J. Org. Chem.* **1992**, *57*, 3759–3760.
[18] a) F. Weinhold, C. R. Landis in *Valency and Bonding: A Natural Bond Orbital Donor-Acceptor Perspective*, Cambridge University Press, New York, **2003**; b) A. E. Reed, L. A. Curtiss, F. Weinhold, *Chem. Rev.* **1988**, *88*, 899–926.

[19] Z. X. Wang, C. G. Zhang, Z. F. Chen, P. v. R. Schleyer, *Inorg. Chem.* **2008**, *47*, 1332–1336.
[20] a) P. v. R. Schleyer, C. Maerker, A. Dransfeld, H.-J. Jiao, N. J. R. E. Hommes, *J. Am. Chem. Soc.* **1996**, *118*, 6317; b) Z. F. Chen, C. S. Wannere, C. Corminboeuf, R. Puchta, P. v. R. Schleyer, *Chem. Rev.* **2005**, *105*, 3842–3888; c) P. v. R. Schleyer, H. Jiao, N. J. R. v. E. Hommes, V. G. Malkin, O. Malkina, *J. Am. Chem. Soc.* **1997**, *119*, 12669–12670.
[21] R. Hoffmann, P. v. R. Schleyer, H. E. Schaefer, *Angew. Chem.* **2008**, *120*, 7276–7279; *Angew. Chem. Int. Ed.* **2008**, *47*, 7164–7167.
[22] H.-G. Lu in GXYZ, Vol. 1, Shanxi University, Taiyuan, **2008**.
[23] S. M. Bachrach, J. V. Miller, *J. Org. Chem.* **2002**, *67*, 7389–7398.
[24] a) A. D. Zdetsis, P. W. Fowler, R. W. A. Havenith, *Mol. Phys.* **2008**, *106*, 1803–1811; b) A. D. Zdetsis, *J. Chem. Phys.* **2007**, *127*, 214306; c) J. C. Santos, P. Fuentealba, *Chem. Phys. Lett.* **2007**, *443*, 439–442.
[25] a) K. Bolton, W. L. Hase, G. H. Peshlherbe, *Modern Methods for Multidimensional Dynamics Computation in Chemistry*, World Scientific, Singapore, **1998**, p. 143; b) W. Chen, W. L. Hase, H. B. Schlegel, *Chem. Phys. Lett.* **1994**, *228*, 436–442; c) J. M. Millam, V. Bakken, W. Chen, W. L. Hase, H. B. Schlegel, *J. Chem. Phys.* **1999**, *111*, 3800–3805; d) X. S. Li, J. M. Millam, H. B. Schlegel, *J. Chem. Phys.* **2000**, *113*, 10062–10067.
[26] X. F. Wang, L. Andrews, *Inorg. Chem.* **2005**, *44*, 610–614.
[27] A. H. Heuer, D. J. Fink, V. J. Laraia, J. L. Arias, P. D. Calvert, K. Kendall, G. L. Messing, J. Blackwell, P. C. Rieke, D. H. Thompson, A. P. Wheeler, A. Veis, A. I. Caplan, *Science* **1992**, *255*, 1098–1105.
[28] a) J. R. Heath, S. C. Obrien, Q. Zhang, Y. Liu, R. F. Curl, H. W. Kroto, F. K. Tittel, R. E. Smalley, *J. Am. Chem. Soc.* **1985**, *107*, 7779–7780; b) *Endofullerenes: A New Family of Carbon Clusters*, Kluwer, Dordrecht, **2002**.
[29] a) E. Osawa, *Kagaku* **1970**, *25*, 854–863; b) D. A. Bochvar, E. G. Galpern, *Acad. Sci. USSR* **1973**, *209*, 239–241; c) R. A. Davidson, *Theor. Chim. Acta* **1981**, *58*, 193–231.
[30] Gaussian 03, Revision E.01, M. J. Frisch, G. W. Trucks, H. B. Schlegel, G. E. Scuseria, M. A. Robb, J. R. Cheeseman, J. A. Montgomery, Jr., T. Vreven, K. N. Kudin, J. C. Burant, J. M. Millam, S. S. Iyengar, J. Tomasi, V. Barone, B. Mennucci, M. Cossi, G. Scalmani, N. Rega, G. A. Petersson, H. Nakatsuji, M. Hada, M. Ehara, K. Toyota, R. Fukuda, J. Hasegawa, M. Ishida, T. Nakajima, Y. Honda, O. Kitao, H. Nakai, M. Klene, X. Li, J. E. Knox, H. P. Hratchian, J. B. Cross, C. Adamo, J. Jaramillo, R. Gomperts, R. E. Stratmann, O. Yazyev, A. J. Austin, R. Cammi, C. Pomelli, J. W. Ochterski, P. Y. Ayala, K. Morokuma, G. A. Voth, P. Salvador, J. J. Dannenberg, V. G. Zakrzewski, S. Dapprich, A. D. Daniels, M. C. Strain, O. Farkas, D. K. Malick, A. D. Rabuck, K. Raghavachari, J. B. Foresman, J. V. Ortiz, Q. Cui, A. G. Baboul, S. Clifford, J. Cioslowski, B. B. Stefanov, G. Liu, A. Liashenko, P. Piskorz, I. Komaromi, R. L. Martin, D. J. Fox, T. Keith, M. A. Al-Laham, C. Y. Peng, A. Nanayakkara, M. Challacombe, P. M. W. Gill, B. Johnson, W. Chen, M. W. Wong, C. Gonzalez, J. A. Pople, Gaussian, Inc., Gaussian, Inc., Pittsburgh PA, **2003**.

Received: July 17, 2009
Published online: November 30, 2009

